MATHEMATICAL ANALYSIS OF FLY FISHING ROD STATIC AND DYNAMIC RESPONSE

DER-CHEN CHANG, GANG WANG, AND NORMAN M. WERELEY

We develop two mathematical models to study the fly fishing rod static and dynamic response. Due to the flexible characteristics of fly fishing rod, the geometric nonlinear models must be used to account for the large static and dynamic fly rod deformations. A static nonlinear beam model is used to calculate the fly rod displacement under a tip force and the solution can be represented as elliptic integrals. A nonlinear finite element model is applied to analyze static and dynamic responses of fly rods.

1. Introduction

The literature of fishing is the richest among all sports and its history dates back to 2000 B.C. The literature of fishing is restrict among any other sports. Even for a subset of fly fishing, much literature is available. However, a significant fraction of fly fishing literature is devoted to its history, rod makers, casting techniques, and so forth. There is a lack of literature about the technology of fly rods in terms of technical rod analysis, rod design, and rod performance evaluation.

In this paper, we will use two different approaches to discuss mathematics for a fly rod based on its geometry and material properties. The first mathematical model is based on the nonlinear equation of a fly rod under a static tip force. The fly rod responses can be solved using an elliptic integrals. The second mathematical model is based on the finite element method, in which a nonlinear finite element model was developed to account for both static and dynamic responses of a fly rod. Typically, a fly rod is considered a long slender tapered beam. The variation of fly rod properties along its length will add complexities to our problem. In this paper, we focus on the presentation of two mathematical models and demonstrate the solution approach. We will continue the follow-up study to provide simplified and accurate solution/formulas for fly rod design and analysis. The paper is based on lectures given by the first author during the International Conference on Differential and Difference Equations which was held at the Florida Institute of Technology, August 1 to 6, 2005. The first author takes great pleasure in expressing his thank

Hindawi Publishing Corporation
Proceedings of the Conference on Differential & Difference Equations and Applications, pp. 287–297

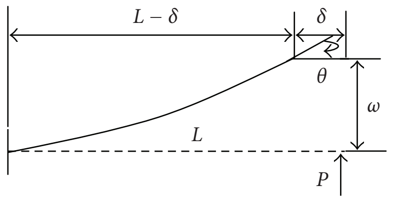

Figure 2.1. Uniform cantilever beam under tip point force.

to Professor Ravi Agarwal for organizing this activity and for the warm hospitality that he received while his visit to Melbourne, Florida.

2. Nonlinear model of fly fishing rod

It was Leonard Euler who first published a result concerning the large deflection of flexible rods in 1744, and it was continued in the Appendix of his book *Des Curvis Elastics*. He stated that for a rod in bending, the slope of the deflection curve cannot be neglected in the expression of the curve unless the deflections are small. Later, this theory was further developed by Jacob Bernoulli, Johann Bernoulli, and L. Euler. The derivation of a mathematical model of a fly rod is based on their fundamental work, which states that the bending moment M is proportional to the change in the curvature produced by the action of the load (see Bisshopp and Drucker [4], also Fertis [6]). Of course, one has to assume that bending does not alter the length of the rod. Now let us consider a long, thin cantilevel leaf spring. Denote L the length of the rod, δ the horizontal component of the displacement of the loaded end of the rod, ω the corresponding vertical displacement, P the concentrated vertical load at the free end, B the flexural stiffness (see Figure 2.1). It is known that

$$B = EI, \tag{2.1}$$

where E is the modulus of elasticity and I is the cross-sectional moment of inertia. If x is the horizontal coordinate measured from the fixed end of the rod, then the product of B and the curvature of the rod equal the bending moment M:

$$B\frac{d\theta}{ds} = P(L-x-\delta) = M \Longleftrightarrow \frac{d^2\theta}{ds^2} = -\frac{P}{B}\frac{dx}{ds} = -\frac{P}{EI}\cos\theta, \tag{2.2}$$

where s is the arc length and θ is the slope angle. It follows that

$$\frac{1}{2}\left(\frac{d\theta}{ds}\right)^2 = -\frac{P}{EI}\sin\theta + C. \tag{2.3}$$

The constant C can be determined by observing that the curvature at the loaded end is zero. If θ_0 is the corresponding slope, then

$$\frac{d\theta}{ds} = \sqrt{\frac{2P}{EI}}\sqrt{\sin\theta_0 - \sin\theta}. \tag{2.4}$$

Since the rod is inextensible, the value of θ_0 can be calculated implicitly as follows:

$$\sqrt{\frac{2PL^2}{EI}} = \sqrt{\frac{2P}{EI}}\int_0^L ds = \int_0^{\theta_0} \frac{d\psi}{\sqrt{\sin\theta_0 - \sin\theta}}. \tag{2.5}$$

Let

$$1 + \sin\theta = 2k^2 \sin^2\psi = (1 + \sin\theta_0)\sin^2\psi. \tag{2.6}$$

Denote

$$\sin\psi_1 = \frac{1}{\sqrt{2}k}, \qquad \gamma^2 = \frac{2PL^2}{EI}. \tag{2.7}$$

Then

$$\begin{aligned}\gamma &= \int_{\psi_1}^{\pi/2} \frac{d\psi}{\sqrt{1 - 2k^2\sin^2\psi}} \\ &= \int_0^{\pi/2} \frac{d\psi}{\sqrt{1 - 2k^2\sin^2\psi}} - \int_0^{\psi_1} \frac{d\psi}{\sqrt{1 - 2k^2\sin^2\psi}} \\ &= K(\sqrt{2}k) - \mathrm{sn}^{-1}\left(\sin\psi_1, \sqrt{2}k\right) \\ &= K(\sqrt{2}k) - F(\psi_1, \sqrt{2}k),\end{aligned} \tag{2.8}$$

where

$$K(k) = \frac{\pi}{2}\left[1 + \left(\frac{1}{2}\right)^2 k^2 + \left(\frac{1\cdot 3}{2\cdot 4}\right)^2 k^4 + \left(\frac{1\cdot 3\cdot 5}{2\cdot 4\cdot 6}\right)^2 k^6 + \cdots\right] \tag{2.9}$$

is the *complete elliptic integral of the first kind* and $F(\psi, k)$ is the Legendre's form of the integral sn^{-1}. Next, one needs to represent the deflection ω in terms of γ and an elliptic integral. Since

$$\frac{dy}{d\theta}\frac{d\theta}{ds} = \frac{dy}{ds} = \sin\theta, \tag{2.10}$$

then we have

$$\frac{dy}{d\theta}\frac{2P}{EI}\sqrt{\sin\theta_0 - \sin\theta} = \sin\theta. \tag{2.11}$$

It follows that

$$\omega = \int_0^y dy = \frac{EI}{2P}\int_0^{\theta_0} \frac{\sin\theta\, d\theta}{\sqrt{\sin\theta_0 - \sin\theta}}. \tag{2.12}$$

Plugging (2.6) into the above equation, one has

$$\frac{\omega}{L} = \frac{1}{\sqrt{2}\gamma}\int_0^{\theta_0} \frac{\sin\theta\, d\theta}{\sqrt{\sin\theta_0 - \sin\theta}} = \frac{1}{\gamma}\int_{\psi_1}^{\pi/2} \frac{(2k^2\sin^2\psi - 1)d\psi}{\sqrt{1 - k^2\sin^2\psi}}. \tag{2.13}$$

It is known that (see Lawden [7])

$$\int_0^{\pi/2} \frac{\sin^2\psi\, d\psi}{\sqrt{1-k^2\sin^2\psi}} = \frac{1}{k^2}(K-E), \tag{2.14}$$

where

$$E = \frac{\pi}{2}\left[1-\left(\frac{1}{2}\right)^2 k^2 - \frac{1}{3}\left(\frac{1\cdot 3}{2\cdot 4}\right)^2 k^4 - \frac{1}{5}\left(\frac{1\cdot 3\cdot 5}{2\cdot 4\cdot 6}\right)^2 k^6 + \cdots\right] \tag{2.15}$$

is the *complete integral of the second kind*. Hence,

$$\int_0^{\pi/2} \frac{2k^2\sin^2\psi\, d\psi}{\sqrt{1-k^2\sin^2\psi}} = \frac{\pi}{2}\left[k^2+\frac{3}{2}\left(\frac{1}{2}\right)^2 k^4+\frac{5}{3}\left(\frac{1\cdot 3}{2\cdot 4}\right)^2 k^6+\frac{7}{4}\left(\frac{1\cdot 3\cdot 5}{2\cdot 4\cdot 6}\right)^2 k^8+\cdots\right]. \tag{2.16}$$

Now we need to look at the term

$$\int_0^{\psi_1} \frac{\sin^2\psi\, d\psi}{\sqrt{1-k^2\sin^2\psi}}. \tag{2.17}$$

After changing variables, this elliptic integral can be expressed as a Jacobi's epsilon function $E(u,k)$ defined by

$$E(\psi_1,k) = \int_0^{\psi_1} \mathrm{dn}^2\, u\, du = \int_0^{\mathrm{sn}\,\psi_1} \sqrt{\frac{1-k^2\,\mathrm{sn}^2\, v}{1-\mathrm{sn}^2\, v}}\,\mathrm{cn}\, v\,\mathrm{dn}\, v\, dv. \tag{2.18}$$

Therefore,

$$\begin{aligned} \frac{\omega}{L} &= \frac{1}{\gamma}\left[2K-2E-E(\psi_1,k)+K(\sqrt{2}k)-F(\psi_1,\sqrt{2}k)\right] \\ &= \frac{1}{\gamma}\left[1-2J-E(\psi_1,k)\right], \end{aligned} \tag{2.19}$$

where

$$J = K-E = k^2\int_0^K \mathrm{sn}^2\, u\, du. \tag{2.20}$$

Now the horizontal displacement of the loaded end can be calculated with $x=0$ and $\theta=0$. It follows that

$$P(L-\delta) = EI\left(\frac{d\theta}{ds}\right)\bigg|_{\theta=0} = \sqrt{2PEI\sin\theta_0} \tag{2.21}$$

or

$$\frac{L-\delta}{L} = \frac{\sqrt{2}}{\gamma}\sqrt{\sin\theta_0}. \tag{2.22}$$

Then from (2.6), one has $\sin\theta_0 = 2k^2 - 1$. We have presented a detailed mathematical solution of beam responses under a tip force. However, in the above solution, a uniform beam with constant flexural stiffness was assumed. Normally it is not valid for a fly fishing rod because it has a tapered shape and the flexural stiffness varies along the rod length. In order to utilize the above elliptic integral solution, we could smear the tapered rod properties and represent it using an equivalent uniform rod. Also, we can account for the flexural stiffness variation and conduct similar elliptic integrals. We will continue such study in a future paper. The goal is to provide a simple engineering solution to fly rod design and analysis. We need to extract and create such simple solution based on the results from elliptic integrals.

3. Finite element method

The key idea is to express the nonlinear strain of deformed configuration in terms of unknown displacements, which are defined with respect to the initial coordinates (see Wang and Wereley [11]). The Newton-Raphson method must be used to iteratively solve for the displacement in the nonlinear finite element model. In the finite strain beam theory, we included the shearing deformation, which leads to the Timosenko beam theory and rotation angle is an independent variable and not equal the slope of transverse displacement. By doing this, we obtain a simple kinematic relationship between strain and displacements. As discussed in Reissner [9], the nonlinear beam axial strain, ε, shear strain, γ, and bending curvature, κ, can be expressed in terms of axial displacement, $u(x)$, transverse displacement, $w(x)$, and rotational displacement, θ, as follows for a straight beam (see also Antman [1]):

$$\begin{aligned}
\varepsilon &= \left(1+\frac{du}{dx}\right)\cos\theta + \frac{dw}{dx}\sin\theta - 1,\\
\gamma &= \frac{du}{dx}\cos\theta - \left(1+\frac{du}{dx}\right)\sin\theta,\\
\kappa &= \frac{d\theta}{dx}.
\end{aligned}\tag{3.1}$$

The next step is to apply the finite element techniques to discretize the beam system. Figure 3.1 shows the two-node geometrically nonlinear finite element based on the finite strain beam theory.

This has been called a geometrically nonlinear Timosenko beam element. The element is not aligned to the x axis for general consideration, which has an initial angel ϕ_0. The nodal degrees of freedom were defined in the fixed frame except that the rotation angles θ_1 and θ_2 were calculated with respect to the initial element orientation. All displacements were linearly interpolated within an element using nodal degrees of freedom

$$\begin{aligned}
u(x) &= N_1(x)U_1 + N_2(x)U_2,\\
w(x) &= N_1(x)W_1 + N_2(x)W_2,\\
\theta(x) &= N_1(x)\theta_1 + N_2(x)\theta_2,
\end{aligned}\tag{3.2}$$

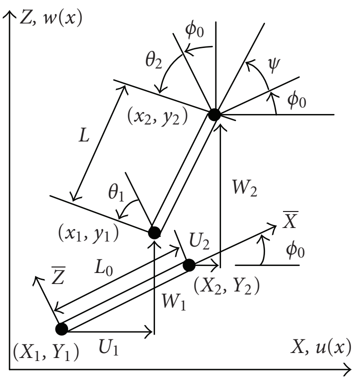

Figure 3.1. Two-node nonlinear finite element based on finite strain beam theory.

where the interpolation functions, $N_1(x)$ and $N_2(x)$, were defined as

$$N_1(x) = 1 - \frac{x}{L}, \qquad N_2(x) = \frac{x}{L}. \tag{3.3}$$

Let us first study the geometric relationships as shown in Figure 2.1. Given the node coordinates at node 1 (X_1, Y_1), and node 2 (X_2, Y_2), the initial reference angle ϕ_0 is determined by

$$\cos\phi_0 = \frac{X_2 - X_1}{L_0}, \qquad \sin\phi_0 = \frac{Y_2 - Y_1}{L_0}, \tag{3.4}$$

where

$$L_0 = \sqrt{(X_2 - X_1)^2 + (Y_2 - Y_1)^2}. \tag{3.5}$$

The angle $\phi_0 + \psi$ can be expressed by

$$\cos(\phi_0 + \psi) = \frac{x_2 - x_1}{L}, \qquad \sin(\phi_0 + \psi) = \frac{y_2 - y_1}{L}, \tag{3.6}$$

where

$$\begin{gathered} x_1 = X_1 + U_1, \qquad x_2 = X_2 + U_2, \qquad y_1 = Y_1 + W_1, \\ y_2 = Y_2 + W_2, \qquad L = \sqrt{(x_2 - x_1)^2 + (y_2 - y_1)^2}. \end{gathered} \tag{3.7}$$

Solving for ψ, one has

$$\begin{aligned} \cos\psi &= \frac{(X_2 - X_1)(x_2 - x_1) + (Y_2 - Y_1)(y_2 - y_1)}{LL_0}, \\ \sin\psi &= \frac{(X_2 - X_1)(x_2 - x_1) - (Y_2 - Y_1)(y_2 - y_1)}{LL_0}. \end{aligned} \tag{3.8}$$

In order to derive the basic stiffness matrices, we need to study the strain and displacement variational relationship

$$\delta\vec{\mathcal{H}} = B\delta\vec{\mathcal{Q}}, \tag{3.9}$$

where δ is a variation operator and $\vec{\mathcal{H}}$ is the strain vector. Here $\vec{\mathcal{Q}}$ is the nodal displacement vector:

$$\mathcal{H} = \begin{bmatrix} \varepsilon & \gamma & \kappa \end{bmatrix}^T, \qquad \mathcal{Q} = \begin{bmatrix} U_1 & W_1 & \theta_1 & U_2 & W_2 & \theta_2 \end{bmatrix}^T. \tag{3.10}$$

The matrix B is calculated by taking partial derivatives of strain vector with respect to nodal displacements which can be written as follows:

$$\begin{bmatrix} \cos(\omega N_1') & \sin(\omega N_1') & N_1\gamma & \cos(\omega N_2') & \sin(\omega N_2') & N_2\gamma \\ -\sin(\omega N_1') & \cos(\omega N_1') & -(1+\varepsilon)N_1 & -\sin(\omega N_2') & \cos(\omega N_2') & -(1+\varepsilon)N_2 \\ 0 & 0 & N_1' & 0 & 0 & N_2' \end{bmatrix}, \tag{3.11}$$

where $\omega = \theta + \phi_0$, ε, and γ are evaluated by

$$\begin{aligned} \varepsilon &= \frac{L\cos\psi\cos\theta + L\sin\psi\sin\theta}{L_0} - 1, \\ \gamma &= \frac{L\sin\psi\cos\theta - L\cos\psi\sin\theta}{L_0}. \end{aligned} \tag{3.12}$$

Here ε and γ are defined in (3.1). Finally, the beam element potential energy based on the finite strain beam theory is

$$\begin{aligned} U &= \frac{1}{2}\int_0^{L_0} \left\{ EA(\tilde{x})\varepsilon^2 + GA(\tilde{x})\gamma^2 + EI(\tilde{x})\left(\frac{d\theta}{d\tilde{x}}\right)^2 \right\} d\tilde{x} \\ &= \frac{1}{2}\int_0^{L_0} \mathcal{P}^T\mathcal{H}\,d\tilde{x}, \end{aligned} \tag{3.13}$$

where G is the shear modulus and $\mathcal{P} = [EA(\tilde{x})\varepsilon \quad GA(\tilde{x})\gamma \quad EI(\tilde{x})\theta']^T$ is the stress resultant vector. For isotropic materials, it can be expressed in terms of Young's modulus, E, and material constant Poisson ratio, ν:

$$G = \frac{E}{2(1+\nu)}. \tag{3.14}$$

The internal nodal force vector can be obtained by taking the first variation of potential energy. Hence,

$$\delta U = \int_0^{L_0} \mathcal{P}^T B\,d\tilde{x} \times \delta\mathcal{Q} \tag{3.15}$$

and the nodal internal force vector is

$$f = \int_0^{L_0} B^T \mathcal{P}^T d\tilde{x}. \tag{3.16}$$

It follows that f is a 6×1 vector. The tangent stiffness matrix can be defined by taking the first variation of internal force vector. Therefore,

$$\delta f = \int_0^{L_0} (B^T \delta\mathcal{P}^T + \delta B^T \mathcal{P}^T) d\tilde{x} = (\mathcal{K}_m + \mathcal{K}_g)\delta\mathcal{Q} = \mathcal{K}\delta\mathcal{Q}. \tag{3.17}$$

The tangent stiffness matrix $\mathcal{K}$ is the sum of material stiffness $\mathcal{K}_m$ and geometric stiffness $\mathcal{K}_g$. It is known that the material stiffness matrix is

$$\mathcal{K}_m = \int_0^{L_0} B^T \begin{bmatrix} EA(\tilde{x}) & 0 & 0 \\ 0 & GA(\tilde{x}) & 0 \\ 0 & 0 & EI(\tilde{x}) \end{bmatrix} B^T d\tilde{x}. \tag{3.18}$$

In order to calculate the geometric stiffness matrix $\mathcal{K}_g$, the important step is to calculate the variation of the matrix B with respect to nodal displacement. From (3.11), we know that the matrix B is a function of ε, γ, and θ. Then B is also a matrix-valued function of nodal displacement. The variation of B with respect to nodal displacements can be calculated by

$$\delta B = \frac{\partial B}{\partial q_j}\delta q_j = B_j \delta q_j, \quad j = 1,\ldots,6. \tag{3.19}$$

After some calculation, the geometric stiffness matrix $\mathcal{K}_g$ can be written as follows:

$$\mathcal{K}_g = \int_0^{L_0} (EA(\tilde{x})\varepsilon B_u + GA(\tilde{x})\gamma B_w) d\tilde{x}, \tag{3.20}$$

where B_u and B_w are 6×6 matrices, and they are assembled using the matrices defined in (3.19) where

$$\begin{aligned} B_u &= \begin{bmatrix} B_1(1,\cdot)^T & B_2(1,\cdot)^T & B_3(1,\cdot)^T & B_4(1,\cdot)^T & B_5(1,\cdot)^T & B_6(1,\cdot)^T \end{bmatrix}, \\ B_w &= \begin{bmatrix} B_1(2,\cdot)^T & B_2(2,\cdot)^T & B_3(2,\cdot)^T & B_4(2,\cdot)^T & B_5(2,\cdot)^T & B_6(2,\cdot)^T \end{bmatrix}. \end{aligned} \tag{3.21}$$

In order to take flexibility of a fly rod during a cast into account, we must include the inertia terms in our nonlinear finite element model. The kinetic energy of a fly rod is

$$T = \frac{1}{2}\int_0^{L_0} \left[\rho A(\tilde{x}) \left(\frac{\partial u}{\partial t}\right)^2 + \rho A(\tilde{x}) \left(\frac{\partial w}{\partial t}\right)^2 + \rho I(\tilde{x}) \left(\frac{\partial \theta}{\partial t}\right)^2 \right] d\tilde{x}, \tag{3.22}$$

where ρ is the density of the fly rod material. Using the same interpolation functions for axial displacement, $u(\widetilde{x})$, transverse displacement, $w(\widetilde{x})$, and rotation angular displacement, $\theta(\widetilde{x})$, we finally obtain the element mass matrix M which is a 6×6 matrix with components

$$\begin{aligned}
M_{11} &= M_{22} = \int_0^{L_0} \rho A(\widetilde{x}) N_1^2 d\widetilde{x}, \\
M_{33} &= \int_0^{L_0} \rho I(\widetilde{x}) N_1^2 d\widetilde{x}, \\
M_{44} &= M_{55} = \int_0^{L_0} \rho A(\widetilde{x}) N_2^2 d\widetilde{x}, \\
M_{66} &= \int_0^{L_0} \rho I(\widetilde{x}) N_2^2 d\widetilde{x}, \\
M_{14} &= M_{41} = M_{25} = M_{52} = \int_0^{L_0} \rho A(\widetilde{x}) N_1 N_2 d\widetilde{x}, \\
M_{36} &= M_{63} = \int_0^{L_0} \rho I(\widetilde{x}) N_1 N_2 d\widetilde{x},
\end{aligned} \tag{3.23}$$

and the rest components are zero. Next, we need to solve the nonlinear dynamic response by using nonlinear finite element approach. The Newton-Raphson equilibrium iteration loop can be used to achieve this goal (see Simo and Vu-Quoc [10] and Newmark [8]). The algorithm of this approach used in our work is listed as follows.

Step 1. Initialize i, $i=0$.

Step 2. Predictor

$$\begin{gathered}
U_{t+\Delta t}^i = U_t, \qquad \ddot{U}_{t+\Delta t}^i = \frac{-1}{\beta\Delta t}\dot{U}_t + \frac{2\beta-1}{2\beta}\ddot{U}_t, \\
\dot{U}_{t+\Delta t}^i = \dot{U}_t + \Delta t\left[(1-\gamma)\ddot{U}_t + \gamma\ddot{U}_{t+\Delta t}^i\right].
\end{gathered} \tag{3.24}$$

Step 3. Increment i, $i=i+1$.

Step 4. Calculate effective stiffness, K_{eff}^i, and residual force vector, Y^i,

$$\begin{gathered}
K_{\text{eff}}^i = \frac{1}{\beta\Delta t^2}M^{i-1} + \frac{\gamma}{\beta\Delta t}D^{i-1} + K_m^{i-1} + K_g^{i-1}, \\
Y^i = R_{\text{ext}}^i - M^{i-1}\ddot{U}_{t+\Delta t}^{i-1} - D^{i-1}\dot{U}_{t+\Delta t}^{i-1} - F_{t+\Delta t}^{i-1}.
\end{gathered} \tag{3.25}$$

Step 5. Solve for displacement increment, $\Delta U^i = (K_{\text{eff}}^i)^{-1}Y^i$.

Table 3.1. Tip vertical displacement results for a tapered cantilevered beam under tip point force.

Taper parameter r	Exact ω [m]	NFEM ω [m]	Error [%]
1.0	18.594	18.586	−0.04
1.2	16.302	16.303	0.00
1.4	13.990	13.995	0.03
1.5	12.881	12.885	0.04
1.6	11.822	11.827	0.05
1.8	9.900	9.905	0.05
2.0	8.264	8.270	0.08
2.2	6.910	6.916	0.09
2.5	5.331	5.337	0.10
3.0	3.580	3.585	0.13

Step 6. Corrector

$$U^i_{t+\Delta t} = U^{i-1}_{t+\Delta t} + \Delta U^i, \qquad \dot{U}^i_{t+\Delta t} = \dot{U}^{i-1}_{t+\Delta t} + \frac{\gamma}{\beta \Delta t}\Delta U^i,$$
$$\ddot{U}^i_{t+\Delta t} = \ddot{U}^{i-1}_{t+\Delta t} + \frac{1}{\beta \Delta t^2}\Delta U^i. \tag{3.26}$$

Step 7. If $\|Y^i\| > 1.0 \times 10^{-5}$, repeat iteration, go to Step 4. Otherwise, $t = t + \Delta t$ and go to Step 1.

The parameter values of $\beta = 0.25$ and $\gamma = 0.5$ were used in our calculation, and D matrix is damping matrix for the fly rod system. We assume that D is the Rayleigh damping matrix and it is expressed as $D = \eta M$ where η is a constant. In order to obtain the convergent and accurate solution, the time step size should be as small as possible. Here we use $\Delta t \leq 1.0 \times 10^{-3}$. The convergence of this process has been discussed by Belytschko-Huges [3] and Argyris-Mlejnek [2]. Similar to the discussion in Chang-Wang-Wereley [5], one can give a mathematical proof of the convergence of this algorithm. Our predictions of tip displacements were compared to those obtained by Fertis [6], as shown in Table 3.1. Here we just list the table of the numerical results for tip vertical displacement results. The beam was 25.4 meters (1000 in) long, and bending stiffness, EI, was assumed to be $EI = 516.21\ N - m^2$ (180×10^3 kip- in^2). The variations of beam moment of inertia and cross-section areas were defined as

$$EI(x) = EI_0\left(r + \frac{1-r}{L}x\right)^3,$$
$$A(x) = A_0\left(r + \frac{1-r}{L}x\right), \tag{3.27}$$

where r is a taper parameter, and cross-section area is assumed as $A_0 = 32.258\ \mathrm{cm}^2$ ($5\ \mathrm{in}^2$), where Poisson's ratio is $\nu = 0$. For a fixed tip loading, $P = 4448.22N$ (1 kip), we calculated tip deflection under different taper rates, or a taper parameter r varying from 1.0 to 3.0. We will give a detailed discussion and comparison of elliptic integrals and finite element solution for the fly rod in a forthcoming paper. A simplified engineering solution will be developed based on the elliptic integral results.

Acknowledgment

This work is partially supported by, under Maryland Industrial Partnerships (MIPs), grant from the Maryland Technology Enterprise Institute (MTECH) and Beaverkill Rod Co.

References

[1] S. S. Antman, *Kirchhoff's problem for nonlinearly elastic rods*, Quarterly of Applied Mathematics **32** (1974), 221–240.

[2] J. Argyris and H.-P. Mlejnek, *Dynamics of Structures*, Texts on Computational Mechanics, vol. 5, North-Holland, Amsterdam, 1991.

[3] T. Belytschko, T. J. R. Hughes, and K.-J. Bathe, *Computational Methods for Transient Analysis*, North-Holland, New York, 1983.

[4] K. E. Bisshopp and D. C. Drucker, *Large deflection of cantilever beams*, Quarterly of Applied Mathematics **3** (1945), 272–275.

[5] D.-C. Chang, T. Nguyen, G. Wang, and N. M. Wereley, *Applications of the Poincaré inequality to extended Kantorovich method*, Journal Inequalities and Applications **2006** (2006), 1–21.

[6] D. G. Fertis, *Nonlinear Mechanics*, 2nd ed., CRC Press, New York, 1999.

[7] D. F. Lawden, *Elliptic Functions and Applications*, Applied Mathematical Sciences, vol. 80, Springer, New York, 1989.

[8] N. M. Newmark, *A method of computation for structural dynamics*, ASCE Journal of Engineering Mechanics **85** (1959), 67–94.

[9] E. Reissner, *On a one-dimensional finite strain beam: the plane problem*, Journal of Applied Mathematics and Physics **23** (1972), no. 5, 795–804.

[10] J. C. Simo and L. Vu-Quoc, *On the dynamics of flexible beam under large overall motions-the plane case: part I and II*, ASME Journal of Applied Mechanice **53** (1986), 849–863.

[11] G. Wang and N. M. Wereley, *Analysis of flexible fly fishing rod and casting dynamics*, Proceedings of IMECE '03, Washington, DC, 2003, pp. 1–8.

Der-Chen Chang: Department of Mathematics, Georgetown University, Washington, DC 20057, USA
E-mail address: chang@georgetown.edu

Gang Wang: Department of Aerospace Engineering, University of Maryland, College Park, MD 20742, USA
E-mail address: gwang@eng.umd.edu

Norman M. Wereley: Department of Aerospace Engineering, University of Maryland, College Park, MD 20742, USA
E-mail address: wereley@eng.umd.edu